Biochemical and Biophysical Research Communications 374 (2008) 90–94

Contents lists available at ScienceDirect

Biochemical and Biophysical Research Communications

journal homepage: www.elsevier.com/locate/ybbrc

Nanostructure and force spectroscopy analysis of human peripheral blood CD4$^+$ T cells using atomic force microscopy

Mingqian Hu [a], Jiongkun Wang [b], Jiye Cai [a,*], Yangzhe Wu [a], Xiaoping Wang [c]

[a] Department of Chemistry, Jinan University, Guangzhou, Guangdong 510632, China
[b] Institution for Tissue Transplantation and Immunology, Jinan University, Guangzhou, Guangdong 510632, China
[c] The First Affiliated Hospital, Jinan University, Guangzhou, Guangdong 510632, China

ARTICLE INFO

Article history:
Received 20 June 2008
Available online 9 July 2008

Keywords:
Atomic force microscopy (AFM)
CD4$^+$ T cells
Morphology
Adhesion force

ABSTRACT

To date, nanoscale imaging of the morphological changes and adhesion force of CD4$^+$ T cells during in vitro activation remains largely unreported. In this study, we used atomic force microscopy (AFM) to study the morphological changes and specific binding forces in resting and activated human peripheral blood CD4$^+$ T cells. The AFM images revealed that the volume of activated CD4$^+$ T cells increased and the ultrastructure of these cells also became complex. Using a functionalized AFM tip, the strength of the specific binding force of the CD4 antigen–antibody interaction was found to be approximately three times that of the unspecific force. The adhesion forces were not randomly distributed over the surface of a single activated CD4$^+$ T cell, indicated that the CD4 molecules concentrated into nanodomains. The magnitude of the adhesion force of the CD4 antigen–antibody interaction did not change markedly with the activation time. Multiple bonds involved in the CD4 antigen–antibody interaction were measured at different activation times. These results suggest that the adhesion force involved in the CD4 antigen–antibody interaction is highly selective and of high affinity.

CD4$^+$ T cells are known to play crucial roles in the immunological control of many viral infections including HIV-1. These cells carry specific CD4 molecules and the biological functions of their antigen–antibody complexes have been well described [1–4]; however, nanoscale imaging of the morphological changes and adhesion force of CD4$^+$ T cells during in vitro activation has not been reported. T cell receptor (TCR) activation occurs upon antigen recognition and may lead to the development of some unique nanostructures after contact with the irritant; these structures may contribute to certain functions such as activation and differentiation [5–8]. We hypothesized that the morphology and adhesion force of CD4$^+$ T cells would be altered after in vitro activation by stimulation, and these changes may have an important effect on the fundamental characteristics of CD4$^+$ T cells. At present, little is known regarding the morphological changes in these cells upon activation and specific adhesion forces involved in the CD4 antigen–antibody interaction. Some researchers studied the morphology of TCRs in vitro using conventional electron microscopy [9]; however, due to the lack of spatial resolution at the nanoscale level, these images could not reveal the ultrastructure and adhesion force of an individual antigen–antibody interaction or the distribution of such forces during clonal expansion–maturation. Nanotechnology-based imaging and force spectroscopy may allow the analysis of TCR nanostructures in the context of T cell recognition of antigens, and the results may provide a new insight into the T cell response and ultimately into immunity.

In the past decade, atomic force microscopy (AFM) [10] has emerged as a powerful tool for obtaining ultrastructural details of biological samples with high resolution [11–13] and for measuring the forces within or between single biomolecules [14–16]. In particular, functionalization of the AFM tip with different ligands has allowed the mapping of complementary receptors on model or cellular surfaces [17,18]. In this article, we report the results of our measurements of the morphological changes and specific binding forces between the CD4 antibody and its receptor using AFM-based single-molecule force spectroscopy. The measurements were carried out on a single resting cell and an activated CD4$^+$ T cell.

Materials and methods

Materials. All reagents used in the experiments were of analytical grade. RPMI-1640 culture medium and fetal bovine serum (FBS) were obtained from Gibco–BRL Corporation. Monoclonal biotinylated anti-human CD4 antibody and biotinylated anti-human CD69 antibody were purchased from eBioscience Corporation. RosetteSep® Human CD4$^+$ T cell enrichment cocktail was purchased from Axis-Shield PoC AS. Biotinylated-bovine serum albumin (BSA) and streptavidin were purchased from Rockland Immunochemicals,

* Corresponding author. Fax: +86 20 8522 3569.
E-mail address: tjycai@jnu.edu.cn (J. Cai).

0006-291X/$ - see front matter © 2008 Elsevier Inc. All rights reserved.
doi:10.1016/j.bbrc.2008.06.107

Inc. Biotin was obtained from Solarbio Science and Technology Co., Ltd. Streptavidin-conjugated QD605 and QD565 and phytohemagglutinin (PHA) were obtained from Sigma Corporation.

Isolation and culture of CD4⁺ T cells. Blood was removed from the peripheral vein of healthy volunteer donors and collected in heparinized test tubes. The RosetteSep Human $CD4^+$ T cell enrichment cocktail was used to enrich $CD4^+$ T cells from whole blood. Highly purified $CD4^+$ T cells (containing more than 90% $CD4^+$ T cells) were inoculated in 24-well tissue culture plates. Each well of the plate contained approximately 2×10^6 cells/ml in 500 μl RPMI-1640 medium. The cells were stimulated with 10 μg/ml PHA and cultured at 37 °C (5% CO_2) for 12, 24, 36, or 48 h.

Confocal microscopy. CD4 and CD69 molecules were viewed under a Carl Zeiss LSM510 Meta Duo Scan laser scanning confocal microscope (LSCM). The staining procedure for mAbs and Qdot conjugates was as follows: $CD4^+$ T cells from the control group were washed three times with PBS and incubated with 10 μg/ml monoclonal biotinylated anti-human CD4 antibody at 4 °C for 20 min. The cells were washed to remove the unbound anti-human CD4 antibody and incubated with 1 μg/ml streptavidin-conjugated QD605 for 30 min. The double staining procedure for the cells in the activation group was similar to that of the control group. Therefore, after staining with streptavidin-conjugated QD605, the cells were blocked with 1 ml biotin (200 μg/ml) at room temperature for 30 min and incubated with 10 μg/ml biotinylated anti-human CD69 at 4 °C for 20 min. These were then incubated with 1 μg/ml streptavidin-conjugated QD565 for 30 min and washed with PBS. The prepared cells were fixed using 4% paraformaldehyde for subsequent experiments.

Functionalization of the AFM tips. Commercially available standard V-shaped Si_3N_4 cantilevers were functionalized with biotinylated anti-human CD4 according to the following procedure [19,20]. The Si_3N_4 tips were immersed in acetone for 5 min and then irradiated with ultraviolet light for 30 min. The irradiated tips were incubated in 50 μl of 1 mg/ml biotinylated BSA (biotin-BSA, 1 mg/ml in 100 mM $NaHCO_3$, pH 9) solution overnight at 37 °C and then rinsed six times with phosphate buffer (PBS: 20 mM Na_2HPO_4, 150 mM NaCl, pH 7.2). Streptavidin was coupled to the tip by incubation with 50 μl of streptavidin (1 mg/ml in PBS) at room temperature for 30 min. After rinsing with PBS to remove any unbound streptavidin molecules, the streptavidin-functionalized tip was immersed in 10 μg/ml monoclonal biotinylated anti-human CD4 antibody solution at 4 °C overnight. The modified tips were stored in PBS at 4 °C for future use.

AFM analysis. An Autoprobe Cp AFM (Thermomicroscope) was used in the contact mode to obtain topographic images. AFM-based force spectroscopy was used for force detection. Force–distance curves were obtained by standard retraction. All force–distance curve experiments were performed at the same loading rate.

Results and discussion

PHA-induced CD4⁺ T cell activation

Slides loaded with QD-stained cells were viewed on an LSCM system equipped with a 63×1.2 oil-immersion objective. Ag/Kr laser beams (488 nm) were used for excitation. Red and green fluorescence emissions were detected through the LP 610 and BP 505–550 filters, respectively, as well as through other filters. Different fluorochromes were scanned sequentially using a multitracking function to avoid any bleed-through of fluorescence emissions (Fig. 1).

Changes in the nanostructure of a single resting cell and an activated CD4⁺ T cell after stimulation for 24 h

To determine whether the morphology of $CD4^+$ T cells was altered by PHA treatment, we examined the cells by AFM. The topographic images revealed a smooth and homogeneous surface in resting $CD4^+$ T cells; the cells had a typical circular shape as expected and were 6–7 μm in diameter and 1.0–1.5 μm in height (Fig. 2A). After treatment with PHA for 24 h, the $CD4^+$ T cells differentiated from both sides, and some pseudopodia were formed around the edges of the cell (Fig. 2E). The mean height of the activated $CD4^+$ T cells increased by approximately twofold, and the diameter became larger than that of the resting cells (approximately 2.0 μm in height and up to 10 μm in diameter). Fig. 2C and G shows the height profile, which was generated along the lines A1–A2 and A3–A4 in Fig. 2A and E, respectively. Comparison of the ultrastructure of the cell membrane surface in a single resting cell with that of an activated $CD4^+$ T cell (Fig. 2B and F, respectively) revealed that the surface of the resting $CD4^+$ T cell was smooth, and no obvious clusters were observed in the topographic image. However, some clusters were observed on the membrane after PHA treatment for

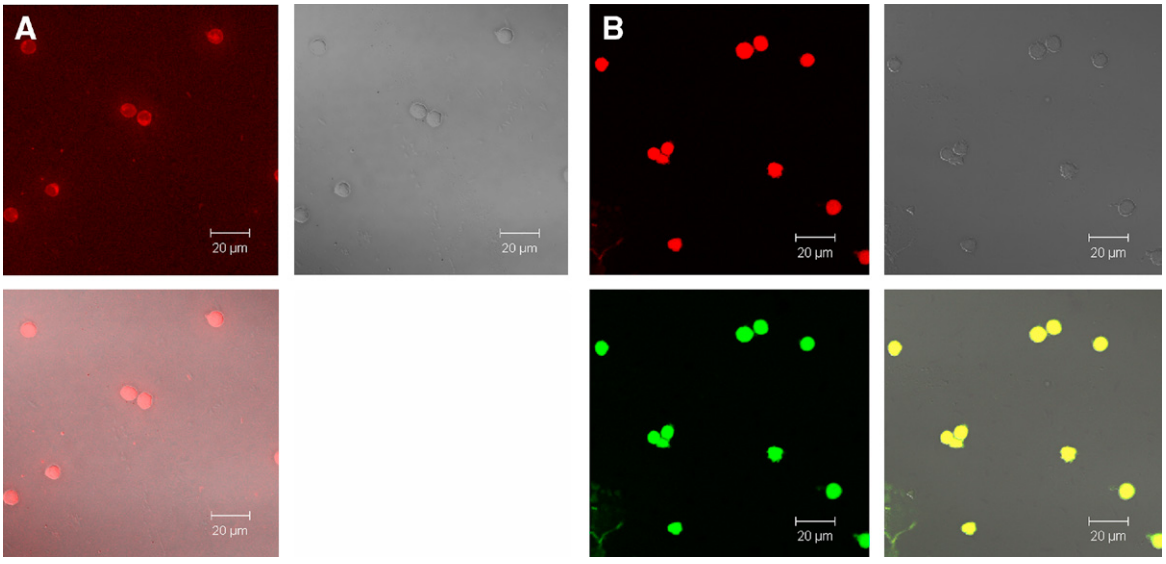

Fig. 1. Representative confocal microscopy data showing PHA-induced $CD4^+$ T cell activation. Resting (A) and activated (B) $CD4^+$ T cells. Red, QD605 + CD4; Green, QD565 + CD69; Yellow, red + green. (For interpretation of the references to color in this figure legend, the reader is referred to the web version of this paper.)

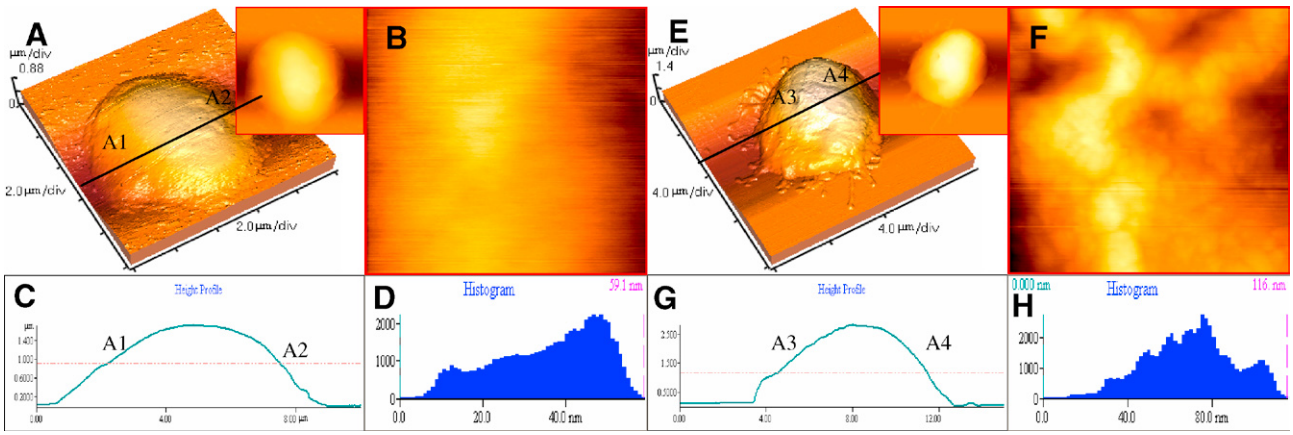

Fig. 2. (A–D) AFM images of a single resting CD4$^+$ T cell. (A) Three-dimensional morphology (size: 10 μm × 10 μm) (inset shows the topological morphology), (B) ultrastructure of the cell membrane surface zoomed from (A) (size: 1 μm × 1 μm), (C) line profile of (A) along the A1–A2 labeled line, and (D) histogram of the particles of (B). (E–H) AFM images of a single activated CD4$^+$ T cell. (E) Three-dimensional morphology (size: 15 μm × 15 μm) (inset shows the topological morphology), (F) ultrastructure of the cell membrane surface zoomed from (E) (size: 1 μm × 1 μm), (G) line profile of (A) along the A3–A4 labeled line, and (H) histogram of the particles of (F).

24 h, as shown in the histograms in Fig. 2D and H. The size of particles in a resting CD4$^+$ T cell was approximately 40 nm, while it increased up to 80 nm in an activated CD4$^+$ T cell.

Mapping of specific force–distance curves of the CD4 antigen–antibody interaction

To determine the force of the CD4 antigen–antibody interaction, the streptavidin–biotin interaction was first chosen for study due to its exceptionally high affinity [21,22]. Biotinylated anti-human CD4 was attached to a streptavidin-functionalized AFM tip, and the CD4 antigen was expressed on the membrane surface of the CD4$^+$ T cells.

All pulling measurements were carried out in a custom-built AFM instrument [23,24]. In this study, we took advantage of AFM force–distance curve analyses to examine the specificity of the CD4 antigen on the membrane surface of CD4$^+$ T cells. In the AFM force–distance curve experiments, the anti-human CD4-functionalized AFM tips allowed the measurement of the single-molecule force involved in the binding of an antibody specific to an antigen on the membrane surface of CD4$^+$ T cells. Typical force–distance curves of the CD4 antigen–antibody interaction are presented in Fig. 3. Resting (Fig. 3 A–D) and activated cells (Fig. 3 E–H) after 24 h are shown in the figure. The retract phase of the force–distance curve is the force required to break the CD4 antigen–antibody bonds formed between the anti-human CD4-functionalized AFM tip and the antigen on the membrane surface (Fig. 3C and G). In contrast, in the control experiments in which unfunctionalized AFM tips were used, no obvious retract phase was observed even when the resting and activated CD4$^+$ T cells were in the same position (Fig. 3D and H). These results suggest that the interactions between the CD4 antigen and its antibody are specific and of high affinity.

We then extended our force–distance analyses to determine the number of functional spots at which CD4 antigens present on the surface of CD4$^+$ T cells were able to specifically capture CD4 antibodies. Fig. 3B and F shows force mapping images on the surface of a single cell using the biotinylated anti-human CD4 tips. We obtained a total of 256 force curves per mapping in a 500 nm × 500 nm area. White spots represent the location where a significant adhesion force was observed between the tip and cell surface. The detectable adhesion force in each spot of this area led to the creation of a map that illustrated the distribution of CD4 antigen spots on the CD4$^+$ T cell. Notably, these spatially resolved adhesion maps revealed that in comparison with the resting cell, the activated CD4$^+$ T cell had a large number of CD4 antigens that were nonuniformly distributed over their surface, but these antigens were apparently concentrated into nanodomains. Only 44% of the coating molecules on the entire CD4$^+$ T cell membrane surface area exposed their high affinity sites in the correct orientation in which they could capture or bind to a specific antibody. These results were qualitatively similar to those obtained by near-field scanning optical microscopy (NSOM) imaging of Vγ2Vδ2 TCR [25] and CD3 [26], in which the molecules were nonuniformly distributed on the surface of T cells, and molecular nanoclusters were not only formed but also sustained on the membrane during activation. The TCR nanoclusters could array to form nanodomains or microdomains on the membrane of clonally expanded Vγ2Vδ2 T cells.

The force–distance scans were performed over five different areas of the sample surface. Interaction among the functionalized AFM tips was observed in all of these, indicating that the observed adhesion forces were due to specific CD4 antigen–antibody interactions and not due to unspecific interactions involving the linker. On the other hand, using the unfunctionalized AFM tips, no obvious interactions were observed in different areas of the sample surface, indicating that the CD4 antigen–antibody interaction was specific. Additionally, AFM crossed experiments between the streptavidin-functionalized tips and a resting or activated CD4$^+$ T cell demonstrated that there were no other forces comparable to those generated by the CD4 antigen–antibody interaction in the force–distance experiments. No obvious interactions were observed either in different areas of the CD4$^+$ T cell surface or in different cells. In other words, the interaction between the CD4 antigen and its antibody appears to be highly selective, which supports the observation that CD4 antigen–antibody interactions could be an additional specific recognition process in nature.

Measurement of multiple bonds in the CD4 antigen–antibody interaction at different activation times

Finally, we examined whether the activation time affected the morphology and force strength of the CD4 antigen–antibody interaction. Therefore, the CD4$^+$ T cells were treated with PHA for 12, 24, 36, and 48 h. The magnitude of the morphological parameters of CD4$^+$ T cells increased significantly with an increase in the activation time. The AFM data showed that there were significant changes in the volume, length, and height of CD4$^+$ T cells after PHA treatment. The rapid change in volume observed by AFM after PHA exposure raises an interesting question of whether the volume increase affects

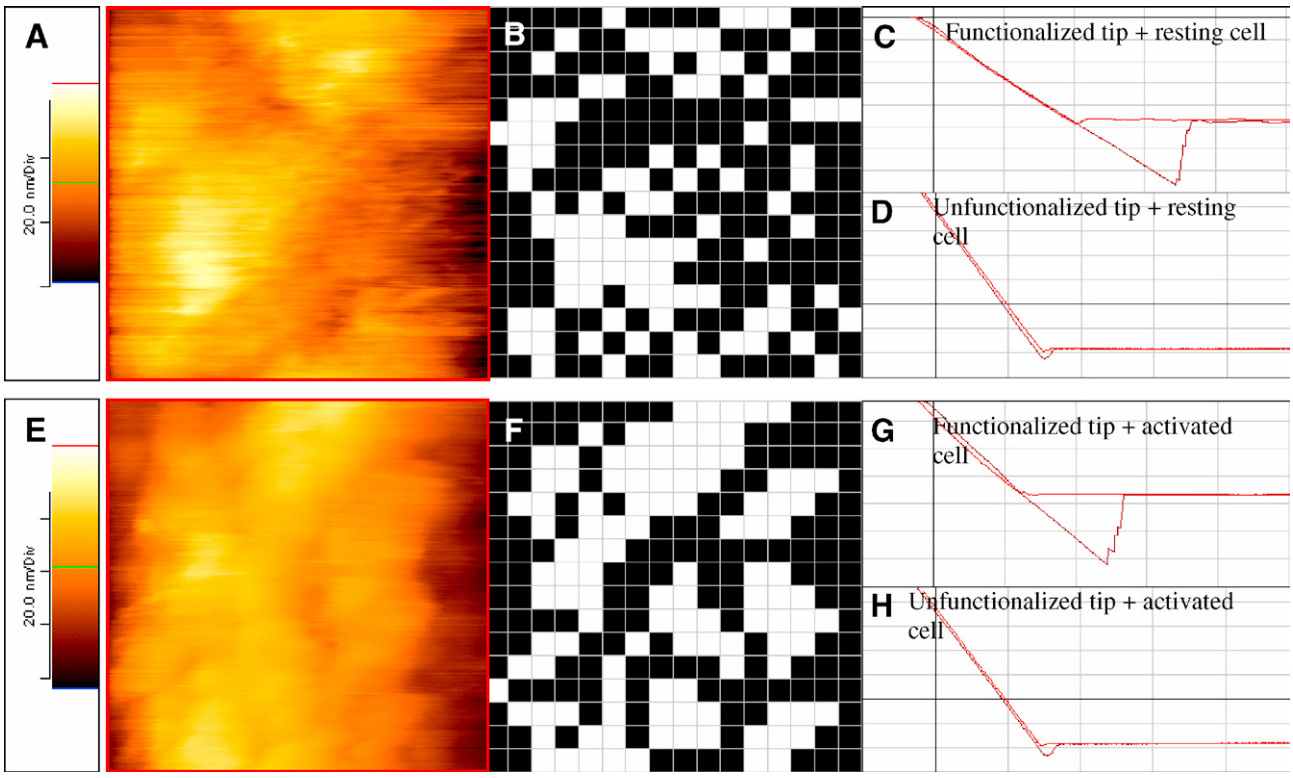

Fig. 3. Nanoscale structure and force curves of $CD4^+$ T cells. (A) High-resolution image of a resting $CD4^+$ T cell surface (size: 500 nm × 500 nm), (B) map of force-curve spots (n=256) recorded using anti-human CD4-functionalized AFM tips ($f_{white} > f_{black}$), (C) the force–distance curve between the functionalized tip and resting cell, and (D) the force–distance curve of the unfunctionalized tip and resting cell. (E–H) High-resolution images (size: 500 nm × 500 nm), map of force-curve spots (n=256) recorded with the anti-human CD4-functionalized AFM tip ($f_{white} > f_{black}$), and the force–distance curve obtained with the functionalized or unfunctionalized AFM tip and an activated $CD4^+$ T cell.

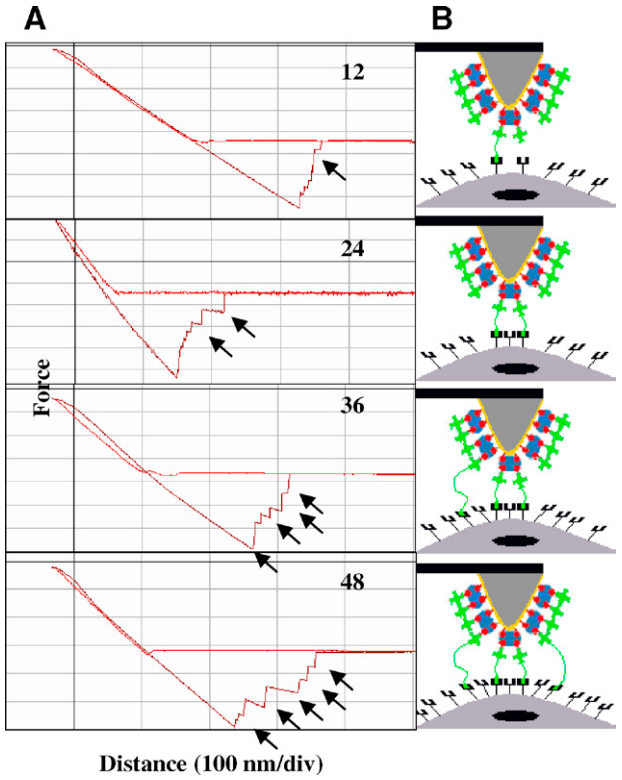

Fig. 4. (A) Measurement of multiple bonds in the CD4 antigen–antibody interaction at different activation times. Arrows point to the breakage of CD4 antigen–antibody bond(s) and (B) a speculative model explaining the stretching phenomenon of the CD4 antigen–antibody interaction at different activation times. Arrows indicate the breakage of CD4 antigen–antibody bond(s).

the strength of the specific CD4 antigen–antibody binding force. Our results indicated that the magnitude of the adhesion force in the CD4 antigen–antibody interaction increases with the activation time, but the increase was not significant. However, AFM studies on multiple bonds provide a wealth of information on a specific antigen–antibody system. As the cantilever is retracted, the bonds formed between the CD4 antigen and antibody are stretched until they begin to break, resulting in the sawtooth profile of the force scan. After breakage of the last bond, the force returns to zero. The force scan of a PHA-treated $CD4^+$ T cell showed that fewer bonds were formed after 12 h of activation than after 24, 36, and 48 h of activation. When PHA was used, there was an even greater increase in the number of bonds formed as well as a large increase in the strength of adhesion and detachment forces, as shown by the arrow in Fig. 4.

This study demonstrated that AFM is a valuable tool for exploring the morphological changes and binding force between an antigen and antibody. Our results provide a better understanding of the morphology, CD4 antigen–antibody binding force, and behavior of $CD4^+$ T cells.

Acknowledgments

This study was supported by the National Natural Science Foundation of China (No. 60578025) and the Key Program of the National Natural Science Foundation of China (No. 30230350).

References

[1] L. Espert, M. Denizot, M. Grimaldi, V. Robert-Hebmann, B. Gay, M. Varbanov, P. Codogno, M. Biard-Piechaczyk, Autophagy is involved in T cell death after binding of HIV-1 envelope proteins to CXCR4, J. Clin. Invest. 116 (2006) 2161–2172.

[2] Y.F. Shi, Y. Feng, J.H. Kang, C. Liu, Z.X. Li, D.S. Li, W. Cao, J. Qiu, Z.L. Guo, E.G. Bi, L. Zang, C.Z. Lu, J.W.Z. Zhang, G. Pei, Critical regulation of $CD4^+$ T cell survival and autoimmunity by β-arrestin 1, Nat. Immunol. 8 (2007) 817–824.
[3] Y. Li, S.A. Migueles, B. Welcher, K. Svehla, A. Phogat, M.K. Louder, X. Wu, G.M. Shaw, M. Connors, R.T. Wyatt, J.R. Mascola, Broad HIV-1 neutralization mediated by CD4-binding site antibodies, Nat. Med. 13 (2007) 1032–1034.
[4] T. Zhou, L. Xu, B. Dey, A.J. Hessell, D. Van Ryk, S.H. Xiang, X. Yang, M.Y. Zhang, M.B. Zwick, J. Arthos, D.R. Burton, D.S. Dimitrov, J. Sodroski, R. Wyatt, G.J. Nabel, P.D. Kwong, Structural definition of a conserved neutralization epitope on HIV-1 gp120, Nature 445 (2007) 732–737.
[5] R. Varma, G. Campi, T. Yokosuka, T. Saito, M.L. Dustin, T cell receptor-proximal signals are sustained in peripheral microclusters and terminated in the central supramolecular activation cluster, Immunity 25 (2006) 117–127.
[6] T. Yokosuka, K. Sakata-Sogawa, W. Kobayashi, M. Hiroshima, A. Hashimoto-Tane, M. Tokunaga, M.L. Dustin, T. Saito, Newly generated T cell receptor microclusters initiate and sustain T cell activation by recruitment of Zap70 and SLP-76, Nat. Immunol. 6 (2005) 1253–1262.
[7] D.D. Billadeau, J.K. Burkhardt, Regulation of cytoskeletal dynamics at the immune synapse: new stars join the actin troupe, Traffic 7 (2006) 1451–1460.
[8] G. Campi, R. Varma, M.L. Dustin, MHC-peptide complex-dependent T cell receptor microclusters as scaffolds for signaling, J. Exp. Med. 202 (2005) 1031–1036.
[9] T. Kuroiwa, K. Nishida, Y. Yoshida, T. Fujiwara, T. Mori, H. Kuroiwa, O. Misumi, Structure, function and evolution of the mitochondrial division apparatus, Biochim. Biophys. Acta 1763 (2006) 510–521.
[10] G. Bennig, C. Quate, C. Gerber, Atomic force microscope, Phys. Rev. Lett. 56 (1986) 930–933.
[11] W.J. Greenleaf, M.T. Woodside, S.M. Block, High-resolution, single-molecule measurements of biomolecular motion, Annu. Rev. Biophys. Biomol. Struct. 36 (2007) 171–190.
[12] J.K.H. Horber, M.J. Miles, Scanning probe evolution in biology, Science 302 (2003) 1002–1005.
[13] Y.F. Dufrêne, Using nanotechniques to explore microbial surfaces, Nat. Rev. Microbiol. 2 (2004) 451–460.
[14] M. Rief, F. Oesterhelt, B. Heymann, H.E. Gaub, Single molecule force spectroscopy on polysaccharides by atomic force microscopy, Science 275 (1997) 1295–1297.
[15] V. Dupres, F.D. Menozzi, C. Locht, B.H. Clare, N.L. Abbott, S. Cuenot, C. Bompard, D. Raze, Y.F. Dufrene, Nanoscale mapping and functional analysis of individual adhesins on living bacteria, Nat. Methods 2 (2005) 515–631.
[16] P. Hinterdorfer, Y.F. Dufrêne, Detection and localization of single molecular recognition events using atomic force microscopy, Nat. Methods 3 (2006) 347–355.
[17] Y. Sugimoto, P. Pou, M. Abe, P. Jelinek, R. Perez, S. Morita, O. Custance, Chemical identification of individual surface atoms by atomic force microscopy, Nature 446 (2007) 64–67.
[18] R. Barattin, N. Voyer, Chemical modifications of AFM tips for the study of molecular recognition events, Chem. Commun. 7 (2008) 1513–1532.
[19] Y. Jin, K. Wang, W. Tan, P. Wu, Q. Wang, H. Huang, S. Huang, Z. Tang, Q. Guo, Monitoring molecular beacon/DNA interactions using atomic force microscopy, Anal. Chem. 76 (2004) 5721–5725.
[20] E.P. Wojcikiewicz, M.H. Abdulreda, X. Zhang, V.T. Moy, Force spectroscopy of LFA-1 and its ligands, ICAM-1 and ICAM-2, Biomacromolecules 7 (2006) 3188–3195.
[21] V.T. Moy, E.L. Florin, H.E. Gaub, Intermolecular forces and energies between ligands and receptors, Science 266 (1994) 257–259.
[22] E.L. Florin, V.T. Moy, H.E. Gaub, Adhesion forces between individual ligand–receptor pairs, Science 264 (1994) 415–417.
[23] G. Zeng, P. Yang, Z. Zheng, Q. Feng, J. Cai, S. Zhang, Z.W. Chen, Nanostructures and molecular force bases of a highly sensitive capacitive immunosensor, Proteomics 5 (2005) 4347–4353.
[24] Y. Chen, Y. Wu, J. Cai, Atomic force microscopic investigation on the potential early intermediate stages of fibrillogenesis of fibronectin within fibrils, Biochem. Biophys. Res. Commun. 361 (2007) 391–397.
[25] Y. Chen, L. Shao, Z. Ali, J. Cai, Z.W. Chen, NSOM/QD-based nanoscale immunofluorescence imaging of antigen-specific T-cell receptor responses during an in vivo clonal Vγ2Vδ2 T-cell expansion, Blood 111 (2008) 4220–4232.
[26] L.Y. Zhong, W.T. Liao, X.P. Wang, J.Y. Cai, Detection the specific marker of CD3 molecules of human peripheral blood T lymphocytes using SNOM and quantum dots, Coll. Surf. A 313 (2008) 642–646.